Single-Ion Two-Photon Source

F. Dubin,[1] D. Rotter,[1] M. Mukherjee,[1] S. Gerber,[1] and R. Blatt[1,2]

[1]*Institute for Experimental Physics, University of Innsbruck, Technikerstrasse 25, A-6020 Innsbruck, Austria*
[2]*Institute for Quantum Optics and Quantum Information of the Austrian Academy of Sciences, Innsbruck, Austria*

A single trapped ion is converted into a pseudo-two-photon source by splitting its resonance fluorescence, delaying part of it and by recombining both parts on a beam splitter. A destructive two-photon interference is observed with a contrast reaching 83(5)%. The spectral brightness of our two-photon source is quantified and shown to be comparable to parametric down-conversion devices.

Light-matter interaction at the quantum scale and its characterization and control have been at the focus of intensive research during many decades. In recent years, the interaction of single atoms with single photons has become more and more important with the goal to experimentally transfer the quantum state between distant sites [1]. While single atoms serve as an ideal quantum memory, for example, as quantum bits (qubits), photons are ideal carriers of quantum information [2] and can also distribute entanglement between qubits [3].

In several recent key experiments various aspects of atom-photon interfacing have been investigated. With atoms trapped in an optical cavity, nearly ideal photon pairs have been produced [4] in a well-controlled polarization state and single photon emission from a single-atom-cavity system [5] has been observed. With pencil-shaped atomic ensembles, single photons have been stored and retrieved with good efficiency [6] thus realizing a photon memory. The state of such a photon memory can also be entangled with the state of the emitted photon [7], and very recently real-time conditional control of two distant atomic quantum memories was achieved through a photonic channel [8].

While atomic ensembles and atom-cavity systems have been demonstrated as photon memories, they usually do not provide optimal conditions for quantum information processing since this demands long coherence times, highly flexible state manipulation and detection schemes. Such features have been demonstrated, in particular, with single trapped ions that allow for nearly perfect control of long lived motional and electronic states. This has been shown recently, for example, by the realization of an entangled state with eight ions in a linear Paul trap [9]. A first milestone toward the interfacing of trapped ions and photons has been demonstrated by entangling the state of fluorescence photons and the internal state of a trapped ion [10]. As a consequent next step, it appears highly attractive to entangle remote trapped ions through a photonic channel.

Two trapped atoms can be entangled at remote sites by the coincident detection of two photons [11], each being entangled with one ion. To this end, photon pairs emitted by two ions confined in the same Paul trap and continuously laser-excited have been measured with a degree of indistinguishability reaching 57% [12] (higher values have been reported [13] during evaluation of this Letter). Under pulsed laser excitation, destructive interference was also observed between photons emitted by two independent atoms in separate dipole traps [14].

Two trapped atoms can also be entangled at remote sites when interacting with narrow-band entangled photon pairs. The latter can, in fact, distribute entanglement [3], with an efficiency limited by the so-called spectral brightness, i.e., "how many photon pairs are produced per second into a particular electromagnetic mode and frequency bandwidth" [4].

In this Letter, we report measurements where the resonance fluorescence of a single trapped ion is split in two parts and then collected in two single mode optical fibers. By delaying one part and then recombining the light, two successively emitted photons may arrive simultaneously at a beam splitter. While single-atom resonance fluorescence exhibits the antibunching property and thus only single photons can be emitted, this setup produces almost ideal two-photon pairs with controlled polarizations. We show that the spectral brightness of our two-photon source is comparable to other sources based on parametric down-conversion [15]. Photon pairs from resonance fluorescence then appear attractive for photon-atom entanglement distribution.

The schematic experimental setup and the relevant level scheme of a $^{138}Ba^+$ ion are shown in Fig. 1. A single Ba^+ ion is loaded in the trap using photo-ionization with laser light near 413 nm [16]. The ion is continuously driven and laser-cooled by two narrow-band (i.e., laser linewidths of a few 10 kHz) tunable lasers at 493 nm (green) and 650 nm (red) exciting the $S_{1/2} - P_{1/2}$ and $P_{1/2} - D_{3/2}$ transitions, respectively. After Doppler cooling, the ion is left in a thermal motional state with a mean number of vibrational excitation $\langle \hat{n} \rangle \approx 15$.

About 1.5% of the green resonance fluorescence is collected with a lens, split in two parts and coupled to
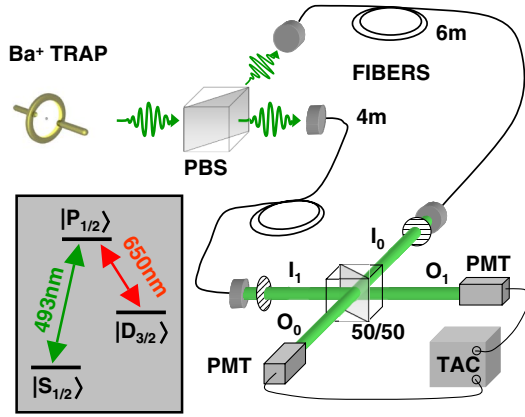
FIG. 1 (color online). Sketch of the experimental setup: A single ^{138}Ba$^+$ ion in a Paul trap is continuously laser excited. Fluorescence photons are collected in two single mode optical fibers via a telescope (not shown). Polarization of the photons is controlled using the combination of a polarizing beam splitter (PBS) and half wave-plates (not shown). At the fiber outputs, photons are vertically polarized by Glan-Thompson polarizers (hatched discs). Single photon arrival times are monitored with a time acquisition card (TAC) with up to 100 ps resolution. The inset shows the relevant electronic levels of ^{138}Ba$^+$ ions.

single mode optical fibers of 4 and 6 m length, respectively. This length difference introduces a time delay $\tau = 10$ ns. The excitation laser parameters (intensity and detuning) are adjusted to produce as many two-photon pairs as possible while an efficient laser cooling is maintained. In fact, one can exploit the Ba$^+$ ion's complex level structure that allows in principle for arbitrary large $g^{(2)}$ values [17]. The polarization at the fiber output is controlled to cancel spurious polarization fluctuations of the fiber transmission. The arrival times of the green fluorescence photons are subsequently monitored and correlated in a Hanbury Brown–Twiss setup with subnanosecond time resolution.

The internal dynamics of a single laser exited atom can be well-characterized by the second order time correlation function of detected fluorescence photons, $g^{(2)}(T)$, i.e., the frequency of time intervals T between detected photons. Since an atom has to be reexcited before it can emit again, for a single atomic emitter the coincidence rate vanishes, i.e., $g^{(2)}(0) = 0$ (antibunching). As was shown by Hong, Ou, and Mandel [18], for two indistinguishable photons impinging at two orthogonal input ports of a beam splitter, photon coalescence is observed. Indistinguishability or the generation of true two-photon states (with a single photon in each input port) is indicated by the vanishing coincidence rate in the output ports of a beam splitter.

Figure 1 shows the experimental setup with the two entrance ports of the 50/50 beam splitter labeled I_0 and I_1 corresponding to the 6 and 4 m fibers, respectively. Incoming photons all have a vertical polarization and the two output ports are denoted O_0 and O_1. Adopting standard notation for the beam splitter transmission ($\mathcal{T}$) and reflection ($\mathcal{R}$) coefficients [19], the field operators in the output

arms 0 and 1 read

$$\hat{E}_{O_0}(t) = \sqrt{\mathcal{T}}\,\hat{E}_i(t - \alpha - \tau) + i\sqrt{\mathcal{R}}\,\hat{E}_i(t - \alpha)e^{i\phi} + N_0(t),$$
(1)

$$\hat{E}_{O_1}(t) = \sqrt{\mathcal{T}}\,\hat{E}_i(t - \alpha)e^{i\phi} + i\sqrt{\mathcal{R}}\,\hat{E}_i(t - \alpha - \tau) + N_1(t).$$
(2)

$\hat{E}_i(t)$ denotes the field emitted by the ion at time t and α takes into account the delay between emission and collection of green photons. The fields at the two input ports have here been directly expressed in terms of $\hat{E}_i$. The phase ϕ corresponds to random fluctuations between the output fields of the two fibers. Although the two output modes are in an identical polarization state and are overlapping with a precision of ≈ 5–$10~\mu$m for the 3 mm beam diameter, the detection setup does not allow for a subwavelength mechanical stability which justifies the introduction of ϕ. Finally, $N_{0,1}(t)$ correspond to the source free part of the input fields [20]. In a frame rotating at the laser frequency ω_L the green photon field radiated by the ion [21] reads

$$\hat{E}_i(t) = \xi e^{-i\omega_L t}\sigma^-(t)\theta(t) + N_i(t),$$
(3)

where ξ represents a constant amplitude and θ is a step function centered at $t = 0$. The lowering Pauli operator from $|P_{1/2}\rangle$ to $|S_{1/2}\rangle$, σ^-, is associated with a single photon creation. The normalized second order correlation, $g^{(2)}(t, t + T) \propto \langle \hat{E}_{O_0}^\dagger(t)\hat{E}_{O_1}^\dagger(t + T)\hat{E}_{O_1}(t + T)\hat{E}_{O_0}(t)\rangle$, can now be evaluated for a vacuum input state [20]. From Eqs. (1)–(3), in the steady state limit ($t \to \infty$) and after averaging over all the possible values for $\phi \in [0, 2\pi]$, we obtain

$$g^{(2)}(T) \propto 2|b_{P_{1/2}}(T)|^2 + |b_{P_{1/2}}(|T - \tau|) - b_{P_{1/2}}(T + \tau)|^2.$$
(4)

$b_{P_{1/2}}$ denotes the occupation amplitude of the $P_{1/2}$ level. It is obtained by solving the time evolution of the ion's internal states, starting in the ground state at $T = 0$. To accurately reproduce the exact shape of the measured correlations, eight relevant electronic sublevels need to be considered [17]. Finally, note that if the two input modes $\hat{E}_{I_0}$ and $\hat{E}_{I_1}$ do not interact, e.g., if they are not spatially overlapping, the normalized correlation function then reads

$$g_{ni}^{(2)}(T) \propto 2|b_{P_{1/2}}(T)|^2 + |b_{P_{1/2}}(|T - \tau|)|^2 + |b_{P_{1/2}}(T + \tau)|^2.$$
(5)

In the following experiments, for a destructive two-photon interference, a mixture of interacting and non-interacting correlations is measured. These have respective weights governed by the interference contrast V, yielding a measured correlation function, $g_{meas}^{(2)}(T) \propto V g^{(2)}(T) + (1 - V)g_{ni}^{(2)}(T)$.

In the inset of Fig. 2 the normalized second order correlation function is presented when one of the two fibers is blocked. The usual single-ion $g^{(2)}$-function is hence measured, with an almost ideal antibunching [$g^{(2)}(0) = 0.02(2)$ with no background subtraction] and a large optical nutation [$g^{(2)}(13 \text{ ns}) = 3.0(3)$].

In Fig. 2 we also present the normalized second order correlation, when the two fiber output modes are not overlapping at the beam splitter, i.e., the noninteracting case. The black line shows the theoretical prediction based on Eq. (5). As expected, photon correlations are well-reproduced by the incoherent superposition of three delayed contributions, centered at $T = 0$ and $T = \pm\tau$, respectively (dashed lines in Fig. 2). Note that we have succeeded in artificially converting a single ion into a bright source of two coincident photons. The number of measured coincidences, $g^{(2)}_{ni}(0) = 1.3(1)$, is indeed higher than the normalization [$g^{(2)}_{ni}(\infty) = 1$], i.e., the average intensity squared.

The normalized second order correlation function for an optimum overlap of the two fiber output modes is presented in Fig. 3. Compared to Fig. 2, a large drop in the coincidence rate is observed with a measured value of 0.21(5). The experimental data are obtained after 30 min of accumulation. In fact, longer integration times limit the contrast of the two-photon interference we measure. A drift of about 5–10% of the interference contrast has been observed within 1–2 h, most likely as a consequence of mechanical instabilities of the interferometer.

For a perfect destructive two-photon interference one would expect $g^{(2)}(0) = 0$. In Eq. (4), the first term (dashed line in Fig. 3) represents the contribution from correlations between photons emerging from the same source (the same fiber in our case). For a single ion or atom this contribution vanishes at $T = 0$. The second term in Eq. (4) (dashed-dotted line in Fig. 3) describes the destructive interference between the amplitudes associated with successive photon detections at times $\{t; t + |T - \tau|\}$ and $\{t; (t + T + \tau)\}$. These two contributions are identical at $T = 0$, consequently the coincidence rate vanishes. The vanishing coincidence rate at $T = 0$ is then the conjoint result of the discrete nature of photon emission (antibunching) and the destructive interference of two-photon state amplitudes. Without the latter, the second order correlation function is not necessarily antibunched (see, for instance, Fig. 2)

In our experiments, detected coincidences have two components: one part is due to accidental correlations between stray-light and fluorescence photons and the other part is given by the fraction of distinguishable photons which are detected. The first contribution is measured to be 3% and is neglected in Fig. 3. The second part derives from imperfect optical alignment such as partial or unmatched mode overlap between the two fiber outputs. Having studied the situation where the two fiber output modes are completely distinguishable—Fig. 2 with $g^{(2)}_{ni}(0) = 1.3(1)$—we conclude that the degree of indistinguishability of the photons we detect, i.e., the two-photon interference contrast (V), is equal to 83(5)% without subtracting accidental counts. Finally, the line shape of the observed two-photon coalescence shows a peculiar statis-
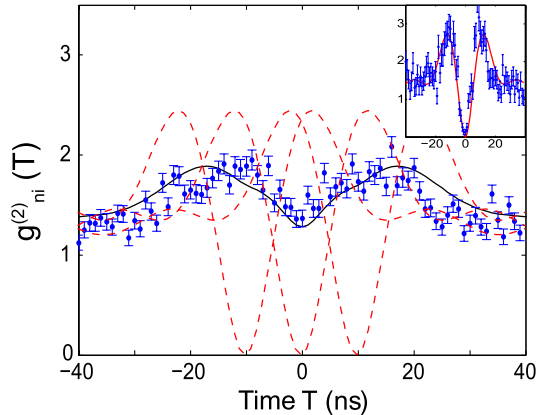

FIG. 2 (color online). Normalized second order correlation function when the two fiber output modes are not overlapping. Data points correspond to an accumulation of 1 h. The black line shows the theoretical prediction $g^{(2)}_{ni}$ using experimental parameters. The dashed lines represent the three delayed correlation functions [Eq. (5)]. Experimental data are presented with a 500 ps resolution and the corresponding variance obtained from shot noise (Poisson statistics at all times T). Inset: Normalized second order correlation function when one fiber output mode is blocked. The line (red online) presents the solution of the Bloch equations for our experimental parameters. Please note the amplitude of the optical nutation.
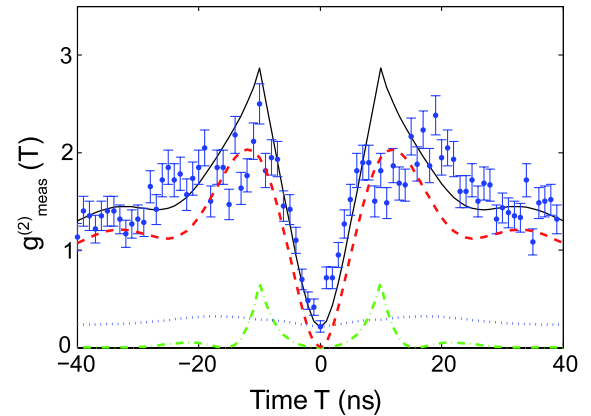

FIG. 3 (color online). Normalized second order correlation function for an optimum overlap between the fiber output modes. Experimental data correspond to 30 min of accumulation. The solid line shows the result of our predictions for $V = 83\%$, i.e., $g^{(2)}_{meas} \propto 0.83 g^{(2)} + 0.17 g^{(2)}_{ni}$. The first contribution splits in two parts: The first term of Eq. (4) shown as the dashed line, and the second term drawn as the dashed-dotted line. Background contributions, i.e., $g^{(2)}_{ni}$, are described by the dotted line. Experimental data are presented with 500 ps resolution and the corresponding variance obtained from shot noise (Poisson statistics at all times T).

tical behavior characterized by the $g^{(2)}$—correlation function, i.e., by the statistics of photon emission. The coherent excitation process shows up as an oscillatory behavior (optical nutation) in the correlation function. The two-photon coalescence reveals a similar effect, as can be seen in Fig. 3 and/or Eq. (4).

Parametric down-conversion (PDC), as the model system for producing entangled photon pairs, is a benchmark for our single-ion two-photon source. PDC photons exhibit a spectral linewidth of the order of 50 GHz [15]. Associated with a rate of $\approx 3 \times 10^6$ pairs/s, a spectral brightness reducing to at most 50 pairs/s per MHz is deduced. In our measurements, a rate of ≈ 1 pair/s is achieved, at a detection rate of $\approx 2 \times 10^4$ photons/channel including all detection losses. Photons elastically scattered by the ion have a linewidth of 10 kHz and then exhibit a spectral brightness about 50 pairs/s per MHz. Inelastically scattered photons have a linewidth of 15.7 MHz yielding a spectral brightness of ≈ 0.1 pairs/s per MHz. This rate can be increased by at least an order of magnitude since the optical nutation in the correlation function can reach ≈ 20 for appropriate laser excitations [17]. Furthermore, in our experiments high numerical aperture halo lenses collecting a total solid angle of 8% are being installed. These should allow enhancement of the spectral brightness by another order of magnitude. Inelastically scattered photon pairs could then reach a spectral brightness of ≈ 20 pairs/s per MHz like typical PDC based devices. However, let us stress that in the experiments reported above, green fluorescence photons are mainly elastically scattered so that the spectral brightness of our two-photon source is ≈ 50 pairs/s per MHz. Moreover, note that the most efficient two-photon source has been demonstrated based on atomic ensembles, with a spectral brightness as high as 5×10^4 pairs/s per MHz [4].

As already mentioned and precisely proposed in Ref. [3], down-converted photon pairs can distribute entanglement between two remote trapped atoms, with an efficiency limited by the spectral brightness. In the same manner, photon pairs obtained from a single-ion delayed resonance fluorescence can also distribute entanglement. In our experiments, successively emitted photons have a controlled polarization and exhibit a high degree of indistinguishability. Setting the polarizers along orthogonal directions (see Fig. 1), photon pairs can be projected in a Bell state at the output of the beam splitter. Associated with proper post-selective detections, such a singlet state could distribute entanglement to two other Barium ions, trapped at distant locations.

In summary, splitting a single-ion resonance fluorescence, delaying part of it, and recombining both parts on a beam splitter allows us to efficiently produce almost ideal two-photon pairs. The adopted experimental configuration reveals that resonance fluorescence photons can be efficiently collected in single mode optical fibers, as required for realizing an extended quantum network. Moreover, the spectral brightness obtained with our current experimental setup is shown to be comparable with current parametric down-conversion devices. Fluorescence photon pairs are therefore potential candidates to achieve entanglement distribution protocols. The success of the last, however, requires a high photon-ion coupling efficiency which can be reached combining an optical cavity and high numerical aperture optical lenses. Thus, our analysis will be of particular interest whenever single atoms and their resonance fluorescence are at the node of quantum networks [1].

[1] P. Zoller *et al.*, Eur. Phys. J. D **36**, 203 (2005); H. J. Briegel *et al.*, Phys. Rev. Lett. **81**, 5932 (1998).
[2] R. Ursin *et al.*, Nature Phys. **3**, 481 (2007).
[3] B. Kraus and I. Cirac, Phys. Rev. Lett. **92**, 013602 (2004).
[4] J. K. Thompson *et al.*, Science **313**, 74 (2006).
[5] T. Wilk *et al.*, Phys. Rev. Lett. **98**, 063601 (2007).
[6] J. Laurat *et al.*, Opt. Express **14**, 6912 (2006); M. D. Eisaman *et al.*, Nature (London) **438**, 837 (2005); T. Chanelière *et al.*, Nature (London) **438**, 833 (2005).
[7] D. N. Matsukevich *et al.*, Phys. Rev. Lett. **95**, 040405 (2005); H. de Riedmatten *et al.*, Phys. Rev. Lett. **97**, 113603 (2006).
[8] D. Felinto *et al.*, Nature Phys. **2**, 844 (2006).
[9] H. Häffner *et al.*, Nature (London) **438**, 643 (2005).
[10] B. B. Blinov *et al.*, Nature (London) **428**, 153 (2004); D. L. Moehring *et al.*, Phys. Rev. Lett. **93**, 090410 (2004).
[11] C. Simon *et al.*, Phys. Rev. Lett. **91**, 110405 (2003).
[12] D. L. Moehring *et al.*, J. Opt. Soc. Am. B **24**, 300 (2007).
[13] P. Maunz *et al.*, Nature Phys. **3**, 538 (2007).
[14] J. Beugnon *et al.*, Nature (London) **440**, 779 (2006).
[15] F. Koening *et al.*, Phys. Rev. A **71**, 033805 (2005).
[16] The photoionization procedure for Barium atoms will be presented elsewhere.
[17] M. Schubert *et al.*, Phys. Rev. A **52**, 2994 (1995).
[18] C. K. Hong Z. Y. Ou, and L. Mandel, Phys. Rev. Lett. **59**, 2044 (1987).
[19] Z. Y. Ou, C. K. Hong, and L. Mandel, Opt. Commun. **63**, 118 (1987).
[20] U. Dorner *et al.*, Phys. Rev. A **66**, 023816 (2002); C. W. Gardiner and P. Zoller, *Quantum Noise* (Springer, Berlin, 2004).
[21] The motion of the ion is here neglected (Lamb-Dicke regime).